Vol 464|25 March 2010|doi:10.1038/nature08899

LETTERS

Zebrafish heart regeneration occurs by cardiomyocyte dedifferentiation and proliferation

Chris Jopling[1], Eduard Sleep[1,2]†, Marina Raya[1]†, Mercè Martí[1], Angel Raya[1,2,3]† & Juan Carlos Izpisúa Belmonte[1,2,4]

Although mammalian hearts show almost no ability to regenerate, there is a growing initiative to determine whether existing cardiomyocytes or progenitor cells can be coaxed into eliciting a regenerative response. In contrast to mammals, several non-mammalian vertebrate species are able to regenerate their hearts[1–3], including the zebrafish[4,5], which can fully regenerate its heart after amputation of up to 20% of the ventricle. To address directly the source of newly formed cardiomyocytes during zebrafish heart regeneration, we first established a genetic strategy to trace the lineage of cardiomyocytes in the adult fish, on the basis of the Cre/*lox* system widely used in the mouse[6]. Here we use this system to show that regenerated heart muscle cells are derived from the proliferation of differentiated cardiomyocytes. Furthermore, we show that proliferating cardiomyocytes undergo limited dedifferentiation characterized by the disassembly of their sarcomeric structure, detachment from one another and the expression of regulators of cell-cycle progression. Specifically, we show that the gene product of *polo-like kinase 1* (*plk1*) is an essential component of cardiomyocyte proliferation during heart regeneration. Our data provide the first direct evidence for the source of proliferating cardiomyocytes during zebrafish heart regeneration and indicate that stem or progenitor cells are not significantly involved in this process.

During heart regeneration in zebrafish, lost ventricular tissue is rapidly replaced. After as little as 1 month, most of the missing tissue has been regenerated by cardiomyocytes. The exact source of these new cardiomyocytes is not yet known definitively. To address this question we developed and successfully implemented the 4-hydroxytamoxifen (4-OHT)-inducible Cre/*lox* approach in zebrafish to label regenerating cardiomyocytes genetically (for a detailed description of the lines generated and/or methodologies, see Methods and Supplementary Figs 1–9).

To examine the contribution made by differentiated cardiomyoctes to regenerated cardiac tissue, we performed a series of amputation experiments on adult zebrafish in which cardiomyocytes had been genetically labelled 48 h after fertilization. About 20% of the ventricle was removed, and cardiac regeneration was subsequently assessed at 7, 14 and 30 days after amputation. At 7 days after amputation, the remaining cardiac tissue was uniformly positive for green fluorescent protein (GFP) (Fig. 1a, b), with much of the missing tissue now replaced by a fibrin/collagen clot ($n = 5$ hearts) (Fig. 1c). At 14 days after amputation, when a significant amount of regeneration had occurred, cardiomyocytes within the regenerating tissue were uniformly GFP-positive (Fig. 1d, e) with only a small fibrin clot remaining ($n = 7$ hearts; Fig. 1f). These results suggest that the regenerated cardiomyocytes arise from differentiated GFP-positive cardiomyocytes. These findings were substantiated at 30 days after amputation, when regeneration is nearly complete; all of the cardiomyocytes within the

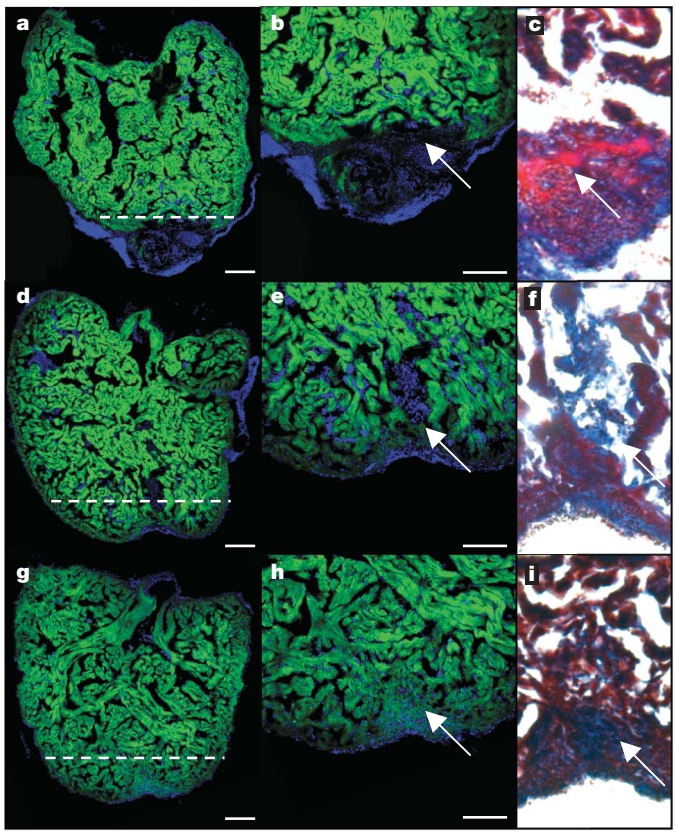

Figure 1 | Regenerated cardiomyocytes are derived from differentiated cardiomyocytes. Cardiomyocytes in transgenic zebrafish (tg-cmlc2a-Cre-Ert2: tg-cmlc2a-LnL–GFP) were genetically labelled at 48 h after fertilization by inducing Cre activity with tamoxifen. These embryos were then grown to adulthood (3 months or sexually mature), at which point the heart was amputated and allowed to regenerate for 7 (**a**–**c**), 14 (**d**–**f**) or 30 (**g**–**i**) days. The dashed white line represents the plane of amputation. At 7 days after amputation (**a**; enlargement in **b**) relatively little regeneration has occurred. Trichromic staining indicates that a fibrin clot has formed adjacent to the wound (**c**). By 14 days after amputation, GFP-positive cardiomyocytes have regenerated a substantial amount of new cardiac tissue (**d**; enlargement in **e**) and the fibrin clot was decreased in size (**f**). At 30 days after amputation, heart regeneration is virtually complete (**g**; enlargement in **h**) and all of the regenerated tissue is composed of GFP-positive cardiomyocytes. The clot has been replaced by a small scar (**h**). Scale bars, 100 μm (**a**, **d**, **g**) and 75 μm (**b**, **e**, **h**). Panels **c**, **f** and **i** are ×2 magnifications of the areas indicated with a white arrow in **b**, **e** and **h**.

[1]Center of Regenerative Medicine in Barcelona, [2]Networking Center of Biomedical Research in Bioengineering, Biomaterials and Nanomedicine (CIBER-BBN), Dr Aiguader Street 88, 08003 Barcelona, Spain. [3]Institució Catalana de Recerca i Estudis Avançats (ICREA), Passeig Lluis Companys 23, 08010 Barcelona, Spain. [4]Salk Institute for Biological Studies, 10010 North Torrey Pines Road, La Jolla, California 92037, USA. †Present addresses: Control of Stem Cell Potency group, Institute for Bioengineering of Catalonia (IBEC), Baldiri Reixac 15, 08028 Barcelona, Spain (E.S., A.R.); Department of Experimental and Health Sciences, Pompeu Fabra University (UPF), Dr Aiguader Street 88, 08003 Barcelona, Spain (M.R.).

regenerated cardiac tissue were clearly GFP-positive ($n = 9$ hearts; Fig. 1g, h).

To determine the overall contribution made by GFP-positive cardiomyocytes to the regenerated heart, at 7, 14 and 30 days after amputation we immunostained regenerating heart sections with anti-GFP and the anti-sarcomeric myosin antibody MF20 (Supplementary Fig. 9a–d). We were unable to detect any cardiomyocytes labelled with MF20 or GFP alone ($n = 4,836$). Taken together, our results demonstrate that, after amputation, the vast majority of newly formed cardiomyocytes, if not all of them, arise from pre-existing cardiomyocytes.

We next sought to determine whether GFP-positive cardiomyocytes had re-entered the cell cycle. Adult GFP-positive transgenic zebrafish were treated with bromodeoxyuridine (BrdU) for 7 days after amputation (Fig. 2a–f). Subsequently, at 14 days after amputation, we found a significant increase in the number of BrdU-positive/GFP-positive cardiomyocytes in regenerating hearts compared with non-amputated controls (Fig. 2g). From this we conclude that differentiated GFP-positive cardiomyocytes had re-entered the cell cycle and engaged in DNA replication. We also analysed the position of BrdU-labelled GFP-positive cardiomyocytes within the regenerating heart (Fig. 2h and inset). Whereas most BrdU-positive/GFP-positive labelled cardiomyocytes were concentrated around the wound, a proportion could also be found in regions far from the site of amputation. This suggests that the response to the injury affects the heart in a global manner.

Recent studies have indicated that cardiomyocytes dedifferentiate to facilitate proliferation, but it is unclear how far within the cardiac lineage they regress[7,8]. An increase in the expression of the cardiac-progenitor-associated genes *nkx2.5* and *hand2* during zebrafish heart regeneration has been reported[9]. However, our own *in situ* hybridization analyses failed to detect any significant upregulation of either transcript (data not shown), confirming previous results from our laboratory[5]. Furthermore, genome-wide transcriptome data[10,11] also failed to detect significant changes in the expression of either transcript during zebrafish heart regeneration. These results argue against an extensive dedifferentiation of cardiomyocytes as a prerequisite for their proliferation in the context of heart regeneration.

To address the extent to which cardiomyocytes dedifferentiate during zebrafish heart regeneration, we analysed regenerating hearts with the use of transmission electron microscopy (TEM). In uninjured hearts (Fig. 3a, b) cardiomyocytes showed an ordered arrangement of sarcomeres and mitochondria with clearly defined Z-lines (Fig. 3b). After amputation, cardiomyocytes began to detach from one another, creating large intercellular spaces (Fig. 3c, d). The aligned array of actin and myosin filaments visible in uninjured hearts (Fig. 3b) became disorganized (Fig. 3d); this was associated with a loss of Z-line structure. Later, at 7 days after amputation (Fig. 3e, f), intercellular spaces were also readily visible as cardiomyocytes detached from one another (Fig. 3e). Furthermore, although sarcomeric filaments were visible, there was a lack of organization leading to the presence of both transverse and longitudinal sarcomeric structures within individual cardiomyocytes (Fig. 3f). Using these criteria, we were able to count the number of cardiomyocytes undergoing phenotypic changes (Supplementary Fig. 10a–c). After

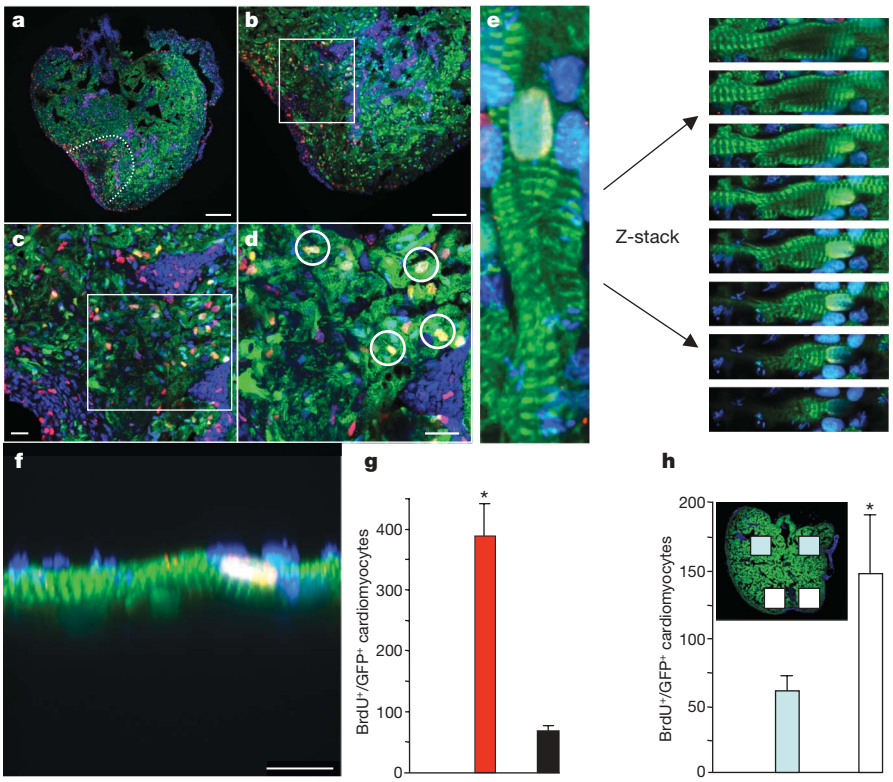

Figure 2 | Differentiated cardiomyocytes re-enter the cell cycle. (**a**–**f**) Transgenic zebrafish (tg-cmlc2a-Cre-Ert2: tg-cmlc2a-LnL–GFP) genetically labelled at 48 h after fertilization and grown to adulthood underwent cardiac amputation and were then treated with BrdU for 7 days after amputation. Hearts were isolated and processed at 14 days after amputation. Green, GFP-positive cardiomyocytes; red, BrdU-positive cells; blue, 4,6-diamidino-2-phenylindole stain for DNA; yellow, BrdU-positive/GFP-positive cardiomyocytes (white rings in **d**). **a**, Section of the entire heart, with a dashed white line representing the regenerating area. **b**, Enlargement of the regenerating area. **c**, **d**, Enlargements of the boxed areas in **b** and **c**, respectively. **e**, An *XY* reconstruction of an individual BrdU-positive/GFP-positive cardiomyocyte within a regenerating heart 14 days after amputation. **f**, An *XZ* reconstruction of the BrdU-positive/GFP-positive cardiomyocyte shown in **e**. **g**, The average number of BrdU-positive/GFP-positive cardiomyocytes per section (means and s.e.m.). Asterisk, $P < 0.01$ (*t*-test). Amputated (red bar), $n = 17$ sections from seven different animals; control (black bar), $n = 9$ sections from three different animals. **h**, The distribution of BrdU-positive/GFP-positive cardiomyocytes ($n = 5$ sections from five different animals). The colours of the bars correspond to the areas indicated in the inset. Scale bars, 100 μm (**a**), 75 μm (**b**) and 10 μm (**c**, **d**, **f**).

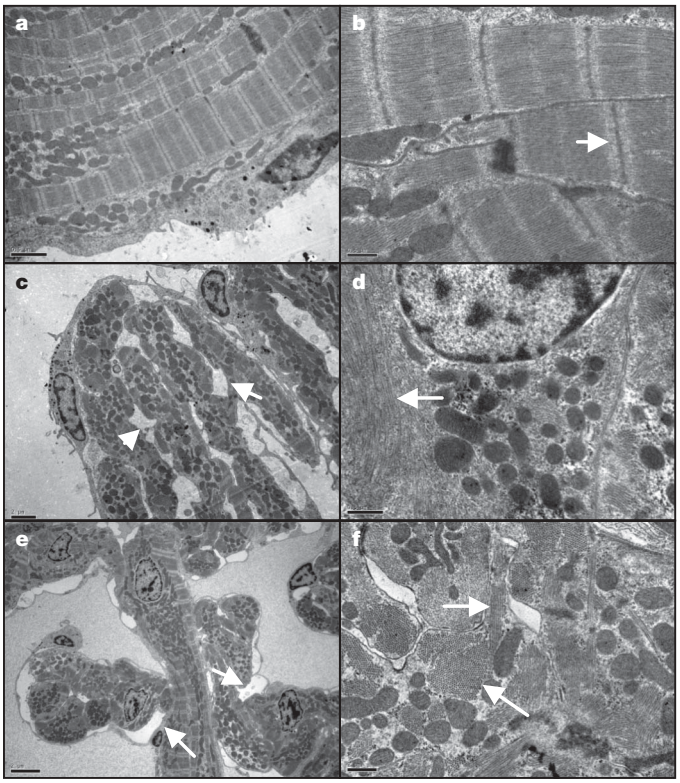

Figure 3 | Cardiomyocytes dedifferentiate, resulting in the disassembly of sarcomeric structure and detachment. Electron microscopy of sections of a control heart (**a**, **b**) and a regenerating heart at 5 days (**c**, **d**) and 7 days (**e**, **f**) after amputation. Cardiomyocytes in unamputated control samples show a tightly organized sarcomeric structure (**a**); at higher magnification (**b**) the Z-lines are clearly visible (arrow). At 5 days after amputation many of the cardiomyocytes have a disorganized sarcomeric structure (**c**) along with the appearance of intercellular spaces (arrows). Closer examination reveals a loss of Z-lines (**d**, arrow). At 7 days after amputation there is a similar loss of structure and appearance of intercellular spaces (**e**, arrows). At higher magnification (**f**) myosin fibres are visible (arrows); however, both longitudinal (upper arrow) and transverse (lower arrow) fibres are present within the same cardiomyocyte, indicating disorganized sarcomeric structure. Scale bars, 0.5 μm (**a**, **b**, **d**) and 2 μm (**c**, **e**, **f**).

amputation, the proportion of these structurally or morphologically altered cardiomyocytes increased, peaking at about day 7 (Supplementary Fig. 10c). Furthermore, their distribution within the regenerating heart closely resembled that of BrdU-labelled cardiomyocytes (Supplementary Fig. 10d and inset). Despite these changes, cardiomyocytes had a healthy appearance and did not show any of the hallmarks associated with cell death[12,13] (Supplementary Fig. 11a–f). TdT-mediated dUTP nick end labelling (TUNEL) of regenerating hearts further confirmed these observations (Supplementary Fig. 12a, b).

The sequence of events described so far indicate that, during regeneration, cardiomyocytes detach from one another and disassemble their sarcomeric structure, presumably to facilitate re-entry to the cell cycle. If this is correct, then cardiomyocytes in the process of cell division should not have any discernible sarcomeric structure. To test this hypothesis we labelled dividing cardiomyocytes with both phosphorylated histone 3 (PH3), a well-established marker of cells undergoing mitosis, and either GFP or MF20. Despite the rarity of these events (an average of three cells per section; $n = 12$ sections from four hearts) none of the PH3-labelled cells showed any discernible organization of their sarcomeric structure (Supplementary Fig. 13a–d). We also immunolabelled GFP-positive cardiomyocytes for proliferating cell nuclear antigen (PCNA) (Supplementary Fig. 14a-c). In a similar manner to PH3-labelled cardiomyocytes, PCNA-positive/GFP-positive cardiomyocytes showed a disorganized sarcomeric structure (Supplementary Fig. 14b, c). These results indicate that the sarcomere is disassembled in the process of cardiomyocyte divison, similarly to the set of events described recently in the mouse[8].

Next we sought to determine whether cardiomyocyte dedifferentiation during heart regeneration was associated with specific changes in gene expression. Previous reports have indicated an increase in expression of the mitotic checkpoint kinase encoded by *mps1* in cardiomyocytes during regeneration and that perturbation of this effectively inhibits regeneration[4]. We therefore examined the expression of *plk1*, which encodes a regulator of cell-cycle progression that was detected as upregulated in previous microarray analyses of zebrafish heart regeneration[11]. *plk1* transcripts were markedly upregulated in regenerating hearts at 1, 3 and 7 days after amputation, as detected by reverse transcriptase-mediated polymerase chain reaction (RT–PCR), closely resembling those of *mps1* (Fig. 4a). In addition, *in situ* hybridization analyses revealed that *plk1* expression increased in cardiomyocytes during regeneration (Fig. 4b, c).

To further assess the role of *plk1* during heart regeneration, we used a recently described embryonic model of heart regeneration[14]. With this model system we were able to ablate cardiomyocytes specifically in embryos at 48 h after fertilization. These were subsequently washed

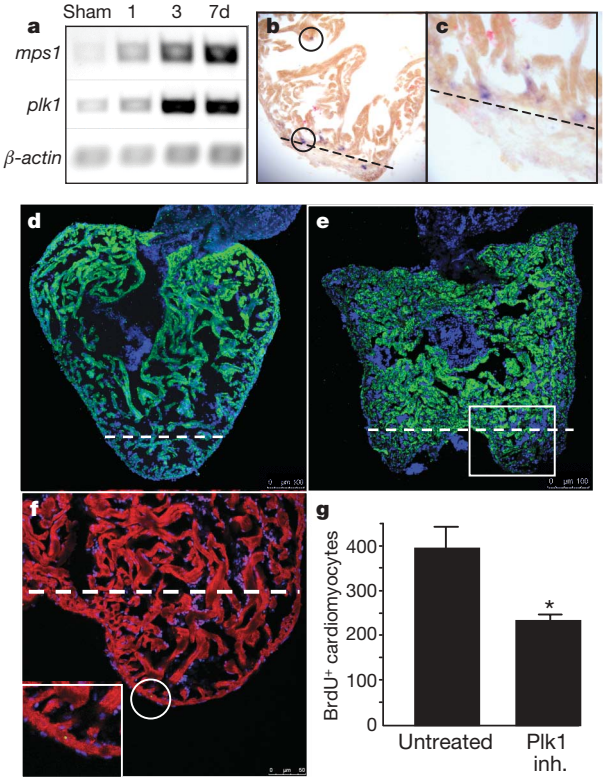

Figure 4 | *plk1* is necessary for cardiac regeneration. **a**, Semi-quantitative RT–PCR of *mps1* and *plk1*. **b**, Double *in situ* hybridization detecting *plk1* mRNA (blue) and *cmlc2a* mRNA (red/brown) in a ventricle 7 days after amputation. The plane of amputation is indicated with a dashed line. **c**, Enlargement of an area shown in **b**. **d**, Regenerating heart at 30 days after amputation (treated with DMSO). The plane of amputation is indicated with a dashed line. **e**, Regenerating heart 30 days after amputation (treated with cyclapolin 9). The plane of amputation is indicated with a dashed line; the white box indicates the area shown in **f**. **f**, Consecutive section taken from the same heart pictured in **e**, labelled with TUNEL (green) and anti-α-sarcomeric actin (red). The plane of amputation is indicated with a dashed line. The inset shows a TUNEL-positive cardiomyocyte. **g**, Plk1 inhibiton decreases the number of cardiomyocytes entering the cell cycle during heart regeneration. The graph indicates the average number of BrdU-positive/GFP-positive cardiomyocytes per section (means and s.e.m.). Asterisk, $P < 0.01$ (*t*-test). Plk1 inhibitor (inh.) (cyclapolin 9) treated, $n = 30$ sections from ten different animals; untreated control, $n = 9$ sections from three different animals. Scale bars, 100 μm (**d**, **e**) and 50 μm (**f**).

and allowed to recover with or without the Plk1 inhibitor cyclapolin 9. In the absence of the inhibitor, 67% of the embryos were able to regenerate their heart. However, in the presence of the inhibitor, this number decreased to 17% (the treatments used in these experiments have no effect on wild-type embryos) (Supplementary Fig. 15a–d). We confirmed these results in the adult setting by inhibiting Plk1 activity with cyclapolin 9 in regenerating zebrafish throughout the 30-day recovery period. Inhibition of Plk1 drastically inhibited the regenerative process (Fig. 4d, e). A TUNEL assay showed that this inhibition was not due to an increase in cardiomyocyte apoptosis (an average of one cell per section; $n = 3$ sections from three different hearts) (Fig. 4f). We also found a significant decrease in the number of BrdU-positive/GFP-positive cardiomyocytes in regenerating animals treated with the inhibitor (Fig. 4g). These results indicate that *plk1* is essential for heart regeneration to proceed.

Overall, our studies show that zebrafish heart regeneration is driven primarily by pre-existing cardiomyocytes, rather than by progenitor cells as suggested previously[9]. The tightness and specificity of our cardiomyocyte lineage-tracing system (Supplementary Figs 1–9; see also Methods) allow us to demonstrate that the vast majority of heart muscle cells, if not all of them, formed during regeneration arise from pre-existing cardiomyocytes. Even though we cannot formally exclude the possibility that stem or progenitor cells may give rise to cardiomyocytes during this process, in the light of our results we can conclude that their contribution to newly formed myocardium would be only marginal. To facilitate proliferation, we found that pre-existing cardiomyocytes undergo limited dedifferentiation. Soon after amputation, cardiomyocytes close to the wound start to disassemble their sarcomeric structure and detach from one another. Furthermore, reduced sarcomeric structure is observed in zebrafish cardiomyocytes re-entering the cell cycle. Microarray analysis also confirms these findings, with many sarcomeric genes being downregulated after amputation[11]. A comparable set of events has also been described in the newt. In that organism the expression of cardiac sarcomeric genes is downregulated after amputation; then, as regeneration proceeds, the expression returns to pre-amputation levels[15]. Similar structural changes are also associated with hibernating myocardium in humans after cardiac injury[16]. Hibernating cardiomyocytes typically show a depletion of sarcomeric structure and an expression pattern of structural proteins closely resembling that in fetal heart cells[17]. Although mammalian cardiomyocytes are unable to regenerate, it is tempting to speculate whether they can complete one of the steps involved in this process. We finally show that, as a prelude to proliferation, zebrafish cardiomyocytes adjacent to the wound begin to express regulators of cell-cycle progression, such as those encoded by *plk1* and *mps1* (ref. 4), which are necessary for the regenerative process to proceed. The fact that zebrafish cardiomyocytes dedifferentiate to a limited extent during heart regeneration, rather than undergoing marked changes in gene expression, offers hope that heart regeneration can also be induced in mammals. In this respect, our studies provide a mechanistic insight into previous findings in mice indicating that forced expression of cell-cycle regulators can induce regeneration after cardiac injury[18].

METHODS SUMMARY

Cardiomyocyte genetic labelling. To induce recombination and subsequently genetically label cardiomyocytes, embryos and adults were treated with 4-OHT followed by a wash period of at least 1 week before amputation.

Zebrafish heart amputation. Adult fish were anaesthetized in 0.4% Tricaine and secured, ventral side uppermost, in a slotted sponge. Watchmaker forceps were used to remove the surface scales and penetrate the skin, muscle and pericardial sac. Once exposed, the ventricle was gently pulled at the apex and cut with iridectomy scissors. After surgery, fish were immediately returned to system water. At the specified time points, hearts were removed and fixed overnight in 4% paraformaldehyde at 4 °C, washed several times in PBS, equilibrated in 30% sucrose in PBS, and frozen for cryosectioning.

Labelling with BrdU. Fish were anaesthetized in 0.4% Tricaine, and 0.5 ml of a 2.5 mg ml^{-1} solution of BrdU (in PBS) was injected into the abdominal cavity once every 24 h for 7 days . After 14 days, hearts were removed and fixed overnight in 4% paraformaldehyde at 4 °C, washed several times in PBS, equilibrated in 30% sucrose in PBS, and frozen for cryosectioning.

Inhibitor treatment. After amputation, adult fish were allowed to recover for 24 h in system water. Cyclapolin 9 (C6493; Sigma) was dissolved in dimethylsulphoxide (DMSO) and added to 400 ml of system water to a final concentration of 3 μM. Water and inhibitor or DMSO alone were changed daily throughout the experimental procedures.

Full Methods and any associated references are available in the online version of the paper at www.nature.com/nature.

Received 31 July 2009; accepted 9 February 2010.

1. Oberpriller, J. O. & Oberpriller, J. C. Response of the adult newt ventricle to injury. *J. Exp. Zool.* **187,** 249–253 (1974).
2. Neff, A. W., Dent, A. E. & Armstrong, J. B. Heart development and regeneration in urodeles. *Int. J. Dev. Biol.* **40,** 719–725 (1996).
3. Flink, I. L. Cell cycle reentry of ventricular and atrial cardiomyocytes and cells within the epicardium following amputation of the ventricular apex in the axolotl, *Amblystoma mexicanum*: confocal microscopic immunofluorescent image analysis of bromodeoxyuridine-labeled nuclei. *Anat. Embryol. (Berl.)* **205,** 235–244 (2002).
4. Poss, K. D., Wilson, L. G. & Keating, M. T. Heart regeneration in zebrafish. *Science* **298,** 2188–2190 (2002).
5. Raya, A. *et al.* Activation of Notch signaling pathway precedes heart regeneration in zebrafish. *Proc. Natl Acad. Sci. USA* **100** (Suppl. 1), 11889–11895 (2003).
6. Dor, Y., Brown, J., Martinez, O. I. & Melton, D. A. Adult pancreatic β-cells are formed by self-duplication rather than stem-cell differentiation. *Nature* **429,** 41–46 (2004).
7. Engel, F. B. *et al.* p38 MAP kinase inhibition enables proliferation of adult mammalian cardiomyocytes. *Genes Dev.* **19,** 1175–1187 (2005).
8. Bersell, K., Arab, S., Haring, B. & Kühn, B. Neuregulin1/ErbB4 signaling induces cardiomyocyte proliferation and repair of heart injury. *Cell* **138,** 257–270 (2009).
9. Lepilina, A. *et al.* A dynamic epicardial injury response supports progenitor cell activity during zebrafish heart regeneration. *Cell* **127,** 607–619 (2006).
10. Lien, C. L., Schebesta, M., Makino, S., Weber, G. J. & Keating, M. T. Gene expression analysis of zebrafish heart regeneration. *PLoS Biol.* **4,** e260 (2006).
11. Sleep, E. *et al.* Transcriptomics approach to investigate zebrafish heart regeneration. *J. Cardiovasc. Med. (Hagerstown)* doi:10.2459/JCM.0b013e3283375900 (22 February 2010).
12. Abbate, A. *et al.* Electron microscopy characterization of cardiomyocyte apoptosis in ischemic heart disease. *Int. J. Cardiol.* **114,** 118–120 (2007).
13. Cheville, N. F. *Ultrastructural Pathology—An Introduction to Interpretation* (Iowa State Univ. Press, 1994).
14. Curado, S. *et al.* Conditional targeted cell ablation in zebrafish: a new tool for regeneration studies. *Dev. Dyn.* **236,** 1025–1035 (2007).
15. Laube, F., Heister, M., Scholz, C., Borchardt, T. & Braun, T. Re-programming of newt cardiomyocytes is induced by tissue regeneration. *J. Cell Sci.* **119,** 4719–4729 (2006).
16. Wijns, W., Vatner, S. F. & Camici, P. G. Hibernating myocardium. *N. Engl. J. Med.* **339,** 173–181 (1998).
17. Dispersyn, G. D., Geuens, E., Ver Donck, L., Ramaekers, F. C. & Borgers, M. Adult rabbit cardiomyocytes undergo hibernation-like dedifferentiation when co-cultured with cardiac fibroblasts. *Cardiovasc. Res.* **51,** 230–240 (2001).
18. Bicknell, K. A., Coxon, C. H. & Brooks, G. Can the cardiomyocyte cell cycle be reprogrammed? *J. Mol. Cell. Cardiol.* **42,** 706–721 (2007).

Supplementary Information is linked to the online version of the paper at www.nature.com/nature.

Acknowledgements We thank M. C. Fabregat, C. Rodriguez Esteban and I. Dubova for technical assistance, and A. Faucherre for constructive criticism of the manuscript. E.S. was the recipient of a pre-doctoral fellowship from the Ministry of Innovation, Universities and Enterprise (DIUE), Generalitat de Catalunya. This work was supported by grants from Fundacion Cellex, the Ipsen Foundation, the G. Harold and Leila Y. Mathers Charitable Foundation, Sanofi-Aventis, the Ministry of Science and Innovation (MICINN), CIBER, and the National Institutes of Health.

Author Contributions C.J., A.R. and J.C.I.B. conceived the project and designed the experiments. C.J. performed the molecular biology and established the transgenic lines. C.J., E.S. and M.R. conducted the experiments. M.M. performed the immunohistochemistry and confocal/transmission electron microscopy imaging. C.J., A.R. and J.C.I.B. wrote the manuscript.

Author Information Reprints and permissions information is available at www.nature.com/reprints. The authors declare no competing financial interests. Correspondence and requests for materials should be addressed to J.C.I.B. (belmonte@salk.edu, izpisua@cmrb.eu).

METHODS

Constructs and zebrafish lines. All constructs were generated with the Tol2 Kit as described[19]. For the tg-cmlc2a-Cre-Ert2 construct the 5′ entry clone *cmlc2a* contained a 1-kilobase PCR fragment of the *cmlc2a* promoter[20], the middle entry clone contained Ert2-Cre-Ert2 amplified from pCAG-ERT2CreERT2 (ref. 21), and the 3′ entry clone contained IRES mCherry.

The tg-cmlc2a-LnL–GFP reporter construct consisted of the *cmlc2a* 5′ entry clone, a middle entry clone containing a floxed stop cassette amplified from pCALNL–GFP[21], and the 3′ entry clone p3E-EGFPpA[19]. Multisite recombination reactions into pDestTol2Pa2 were performed as described[19].

The NTR–GFP fusion construct was generated by using the *cmlc2a* 5′ entry clone, a middle entry clone pME–EGFP 'no stop', and a 3′ entry clone containing *nitroreductase* amplified from pECFP-*Nitro* (ref. 14). Multisite recombination reactions into pDestTol2Pa2 were performed as described[19].

The Ert–GFP construct was generated by using a 5′ entry clone p5E-*bactin2* (ref. 19), a middle entry clone containing Ert2 fused to GFP amplified from pErt2–GFP (pErt2–GFP was generated by cloning Ert2 from pCAG-ERT2CreERT2 (ref. 21) into the *Eco*R1 and *Bam*H1 sites of pEGFP-N1 (Clontech)), and a 3′ entry clone containing Ert2 amplified from pCAG-ERT2CreERT2 (ref. 21). Multisite recombination reactions into pDestTol2Pa2 were performed as described[19].

To generate stable transgenic lines the tg-cmlc2a-Cre-Ert2 and tg-cmlc2a-LnL–GFP plasmids were injected into one-cell-stage embryos with transposase RNA[19].

Cre/tamoxifen in zebrafish. Transgenic zebrafish were generated in which 4-OHT-inducible Cre is under the control of the cardiomyocyte-specific *cmlc2a* promoter[20]. Concomitantly, the reporter construct used the same *cmlc2a* promoter followed by a floxed stop cassette and enhanced green fluorescent protein (EGFP). Removal of the stop cassette by Cre allows the *cmlc2a* promoter within the transgene to drive the expression of GFP. Subsequently, any cell derived from these GFP-positive cardiomyocytes will also be genetically labelled and will therefore also express GFP. However, cells in which the *cmlc2a* promoter was silent at the time of 4-OHT treatment (for example progenitor cells), would not have expressed any Cre and therefore the reporter in these cells will not be recombined and will remain silent. Any cell derived from these unlabelled cells will also remain unlabelled. To test the efficacy of this system, embryos from a heterozygous incross were treated with a range of concentrations of 4-OHT (H7904; Sigma). We found that 2 μM 4-OHT is sufficient to produce an efficient Cre-mediated recombination of the floxed stop cassette and subsequent uniform expression of GFP in cardiomyocytes (Supplementary Fig. 1a, b). Before treatment with 4-OHT, embryos show no discernible expression of GFP (Supplementary Fig. 1a), indicating that this system does not leak. At 24 h after treatment with 4-OHT, cardiomyocytes in the embryonic heart express GFP (Supplementary Fig. 1b) with no discernible ectopic expression, demonstrating the specificity of the tg-cmlc2a-Cre-Ert2/cmlc2a-LnL–GFP line. Consequently, treated embryos were grown to adulthood (3 months or sexually mature), at which stage cardiomyocytes within the heart are still uniformly GFP-positive (Supplementary Fig. 1c). Similar findings with this system have also been recently reported[22,23]. Furthermore, examination of cells isolated from GFP-positive transgenic hearts shows that all GFP-positive cells are MF20-positive ($n = 999$) (Supplementary Fig. 2a–d). The specificity of Cre-Ert2 expression in the tg-cmlc2a-Cre-Ert2 line was directly tested by crossing these fish with animals from two different ubiquitous Cre reporter lines ((Tg(eab2:[EGFP-T-mCherry])[23] and EF1α loxP-DsRed2-loxP EGFP[22]; gifts from W. Chen and M. Brand, respectively). Zebrafish embryos from either intercross displayed strong reporter activation in the heart, and no ectopic expression was detected after detailed analyses with ultraviolet and confocal microscopy (Supplementary Figs 3 and 5). Identical results were also obtained by crossing a second tg-cmlc2a-Cre-Ert2 line with the EF1α loxP-DsRed2-loxP EGFP line (Supplementary Fig. 6a–j). Analyses of regenerating hearts from this second tg-cmlc2a-Cre-Ert2 line indicate that all the regenerated cardiac tissue is GFP-positive (Supplementary Fig. 6k). These findings decrease the chance of mislabelling to negligible levels. To further ensure that Cre-Ert2 expression was restricted to cardiomyocytes, embryos from the tg-cmlc2a-Cre-Ert2/Tg(eab2:[EGFP-T-mCherry]) analysis detailed above were raised until 2 months old. We subsequently isolated hearts from these animals and performed immunohistochemistry with anti-red fluorescent protein (anti-RFP; to label mCherry-expressing cells) and anti-α-sarcomeric actin (to label cardiomyocytes). We were unable to detect any cells labelled with anti-RFP alone ($n = 1{,}564$), indicating that Cre expression is restricted to cardiomyocytes (Supplementary Fig. 4a–c). Furthermore, we isolated cells from tg-cmlc2a-Cre-Ert2/Tg(eab2:[EGFP-T-mCherry]) transgenic hearts and found that all mCherry-positive cells were also positive for α-sarcomeric actin ($n = 843$) (Supplementary Fig. 4d–f). This confirms that Cre expression is restricted to cardiomyocytes.

Next we sought to determine whether this system was also effective in adult fish. Untreated GFP-negative embryos were raised to adults and then outcrossed to wild-type zebrafish. Embryos from this outcross were treated with 4-OHT to induce GFP expression in the heart, allowing us to identify the positive transgenic adults (Supplementary Fig. 1d and inset). Before treatment with 4-OHT, transgenic adult fish show no GFP expression in the heart (Supplementary Fig. 1d), again indicating no leakage. Previous findings have proposed that under certain conditions reporter systems such as those using the heat shock promoter can become inadvertently activated. However, we found no expression of GFP in cardiomyocytes after heart amputation (7-day recovery) in adult transgenics, indicating that even after a stressful procedure the reporter remains silent (Supplementary Fig. 1e and inset). To induce the expression of GFP in cardiomyocytes, adult transgenics were treated every 2 days with 1 μM 4-OHT for 1 week followed by a 1-week wash period after which GFP is readily visible in cardiomyocytes (Supplementary Fig. 1f). To rule out the possibility that labelling cardiomyocytes at embryonic stages also resulted in labelling of progenitor cells, GFP-negative transgenic fish were treated with 4-OHT as adults and subsequently amputated. At 30 days after amputation we assessed regeneration and found again that all cardiomyocytes within the regenerate were GFP-positive (Supplementary Fig. 8a, b).

To establish that Cre is removed from the nucleus after 4-OHT withdrawal, we fused the same oestrogen receptors to GFP (GFP–ER) allowing us to reveal, *in vivo*, the dynamics of 4-OHT treatment. Under the control of the *β-actin* promoter and in the presence of 4-OHT, GFP–ER is concentrated in the nucleus of a variety of cells in embryonic zebrafish (Supplementary Fig. 7a). Three days after 4-OHT withdrawal, GFP–ER returns to its pre-treatment cytoplasmic status (Supplementary Fig. 5b), similar to time windows established in the mouse (between 2 and 4 days until removal from nucleus)[6,24].

Amputation. Amputations were performed as described previously[5].

Inhibitor treatments. Cyclapolin 9 (C6493; Sigma) was dissolved in DMSO and added to 400 ml of system water to a final concentration of 3 μM. Water and inhibitor or DMSO alone were changed daily throughout the experimental procedures.

Labelling with BrdU. Treatment with BrdU was performed essentially as described[5]. Metamorph software (Molecular Devices) was used to count the total number of BrdU-labelled cardiomyocytes in each section (17 regenerating sections from 7 different animals, and 9 control sections from 3 animals).

Cardiomyocyte islolation. Fish were killed in Tricaine and injected intraperitoneally with 20 μl of a 1,000 U ml^{-1} heparin solution in PBS to avoid blood clotting on heart extraction. Hearts were collected and placed in PBS containing penicillin and streptomycin and 10 U ml^{-1} heparin. The outflow tracts were then removed, and ventricles and atria were opened to get rid of the blood. They were then washed three times in perfusion buffer (PBS containing 10 mM HEPES, 30 mM taurine, 5.5 mM glucose and 10 mM 2,3-butanedione monoxime (BDM)) and placed in digestion buffer (perfusion buffer plus 12.5 μM calcium chloride and 0.2 Wünsch units ml^{-1} Liberase Blendzyme 3 (Roche)) to digest for 40 min at 27 °C in a Thermomixer at 800 r.p.m. Next, an equal volume of stop buffer 1 (perfusion buffer plus 12.5 μM calcium chloride and 10% FBS) was added and cells were separated mechanically. Undigested material was left to sediment and cells suspended in the supernatant were pelleted by centrifugation at 250*g* for 5 min. The cells were then resuspended in stop buffer 2 (perfusion buffer plus 12.5 μM calcium chloride and 5% FBS), and calcium reintroduction was performed by gradually increasing the concentration to 62, 112, 212, 500 and 1,000 μM. Cells were then pelleted again and resuspended in plating medium (MEM containing 5% FBS, 10 mM BDM, 2 mM Glutamax, 100 U ml^{-1} penicillin and 100 μg ml^{-1} streptomycin). Undigested material was washed once in perfusion buffer, digested and subsequently treated again following the same steps as described previously. Both cell preparation batches were combined, plated onto Matrigel-coated chamber slides (177445; Nunc), and allowed to attach overnight. Immunofluorescence was performed the following day.

Immunohistochemistry. Immunohistochemistry was performed on 10 μm cryosections as described previously[4]. The antibodies used in this study were MF20 (DSHB), anti-GFP (GFP-1020; Aves Labs), anti-BrdU (OBT0030; Accurate Chemical), anti-phospho-histone H3 (06-570; Upstate), TUNEL (11684817910; Roche), anti-PCNA (P8825; Sigma), anti-α-sarcomeric actin (A2172; Sigma) and anti-RFP (ab34771; Abcam).

***In situ* hybridization.** *In situ* hybridization was performed as described previously[5]. The *plk1* probe was generated by cloning zebrafish *plk1* from RZPD clone IRBOp991A0269D into the *Eco*R1 and *Xho*1 sites of pBSK− .

Semithin-section analysis. For each section, six images were taken in the positions indicated in Supplementary Fig. 10d inset. Structurally altered cardiomyocytes were identified manually with Metamorph software (Molecular Devices). Each time point in Supplementary Fig. 10c represents the average of all six images (mean ± s.e.m.). For 3 and 7 days after amputation, four sections were analysed from two different hearts. For control, 1 day, 14 days and 30 days after amputation,

four sections were analysed from one heart for each time point. For positional analysis (Supplementary Fig. 10d) the average was taken from positions 1 + 2 and 5 + 6 from all the sections 3 and 7 days after amputation.

Confocal microscopy. Confocal microscopy was performed with a Leica SP5. For co-localization analysis the formula used to calculate the axial resolution (D_z) is as follows.

$$D_z = \sqrt{\{[l \times n/(\mathrm{NA})^2] + [\mathrm{AU} \times n \times \sqrt{2} \times 1.22 \times l/(\mathrm{NA})^2]^2\}}$$

$$\text{Emission } (l) = 500\,\text{nm}$$

$$\text{Refractive index } (n) = 1.518$$

$$\text{Numerical aperture (NA)} = 1.4$$

$$\text{Airy units (AU)} = 1$$

This results in a section thickness of $z = 0.773\,\mu\text{m}$.

Transmission electron microscopy. Transmission electron microscopy was performed as described previously[25].

19. Kwan, K. M. *et al.* The Tol2kit: a multisite gateway-based construction kit for Tol2 transposon transgenesis constructs. *Dev. Dyn.* **236,** 3088–3099 (2007).
20. Huang, C. J., Tu, C. T., Hsiao, C. D., Hsieh, F. J. & Tsai, H. J. Germ-line transmission of a myocardium-specific GFP transgene reveals critical regulatory elements in the cardiac myosin light chain 2 promoter of zebrafish. *Dev. Dyn.* **228,** 30–40 (2003).
21. Matsuda, T. & Cepko, C. L. Controlled expression of transgenes introduced by *in vivo* electroporation. *Proc. Natl Acad. Sci. USA* **104,** 1027–1032 (2007).
22. Hans, S., Kaslin, J., Freudenreich, D. & Brand, M. Temporally-controlled site-specific recombination in zebrafish. *PLoS ONE* **4,** e4640 (2009).
23. Boniface, E. J., Lu, J., Victoroff, T., Zhu, M. & Chen, W. FlEx-based transgenic reporter lines for visualization of Cre and Flp activity in live zebrafish. *Genesis* **47,** 484–491 (2009).
24. Boyle, S. *et al.* Fate mapping using Cited1-CreERT2 mice demonstrates that the cap mesenchyme contains self-renewing progenitor cells and gives rise exclusively to nephronic epithelia. *Dev. Biol.* **313,** 234–245 (2008).
25. Glauert, A. M. *Practical Methods in Electron Microscopy* (Elsevier North-Holland, 1974).